

Memory-Maze: Scenario Driven Benchmark and Visual Language Navigation Model for Guiding Blind People

Masaki Kuribayashi^{*1}, Kohei Uehara^{*2}, Allan Wang³, Daisuke Sato³, Simon Chu³, Shigeo Morishima⁴

Abstract—Visual Language Navigation (VLN) powered navigation robots have the potential to guide blind people by understanding and executing route instructions provided by sighted passersby. This capability allows robots to operate in environments that are often unknown a priori. Existing VLN models are insufficient for the scenario of navigation guidance for blind people, as they need to understand routes described from human memory, which frequently contain stutters, errors, and omission of details as opposed to those obtained by thinking out loud, such as in the Room-to-Room dataset. However, currently, there is no benchmark that simulates instructions that were obtained from human memory in environments where blind people navigate. To this end, we present our benchmark, Memory-Maze, which simulates the scenario of seeking route instructions for guiding blind people. Our benchmark contains a maze-like structured virtual environment and novel route instruction data from human memory. To collect natural language instructions, we conducted two studies from sighted passersby onsite and annotators online. Our analysis demonstrates that instructions data collected onsite were more lengthy and contained more varied wording. Alongside our benchmark, we propose a VLN model better equipped to handle the scenario. Our proposed VLN model uses Large Language Models (LLM) to parse instructions and generate Python codes for robot control. We further show that the existing state-of-the-art model performed suboptimally on our benchmark. In contrast, our proposed method outperformed the state-of-the-art model by a fair margin. We found that future research should exercise caution when considering VLN technology for practical applications, as real-world scenarios have different characteristics than ones collected in traditional settings.

I. INTRODUCTION

A visual language navigation (VLN) task is a task where an agent with access to visuals of the surroundings navigates under a human’s instructions [1]. Recently, navigation robots for blind people have been developed to help them gain independence [2], [3], [4], [5], such as robots that allow users to choose destinations within prebuilt maps [2], [4], [3]. One scenario in which such robots would benefit from the VLN technology is where blind people request instructions to their destinations from sighted passersby in unfamiliar buildings [6]. In this scenario, the VLN technology deployed on navigation robots may assist their blind users by understanding verbal instructions from the passersby and then autonomously guiding them to their destinations. VLN technology could also allow robots to operate autonomously without relying on building infrastructure or prebuilt maps,



Fig. 1. The overview of the virtual environment, Memory-Maze based on CARLA [7] (the ceiling and some walls are removed for visibility).

which is crucial for allowing robots to assist blind people in navigating various new environments.

However, the direct application of existing VLN models to the scenario is currently limited, as there is a need for a benchmark (*i.e.*, a virtual environment with instruction data) that reflects the blind users’ demands realistically. Many VLN tasks have been addressed in environments such as static houses [1] or roadways [8]. Nonetheless, it is most important for blind individuals to navigate public spaces such as shopping malls or university hallways. Such environments are characterized by physical turning points and intersections, resembling a very simple maze, compared to previous environments. Large public areas also contain both static and dynamic obstacles and vary in their environmental structures. Besides the environmental difference, in existing VLN literature, natural language instructions are provided by thinking out loud. In other words, annotators visually navigate a virtual environment and type out instructions for constructing routes concurrently. In our unique scenario, sighted passersby must describe the route from their memory, which often contains errors such as inaccurate estimates of distances, hallucinations of landmark objects, and omissions of key turning points. To the best of our knowledge, our benchmark is the first to address the scenario of a blind user seeking instructions from sighted passersby in public spaces characterized by turning points.

We present *Memory-Maze*, a benchmark that reflects the blind user navigation scenario. Memory-Maze contains a

^{*} Equal Contribution ¹Waseda University ²Miraikan - The National Museum of Emerging Science and Innovation ³Carnegie Mellon University ⁴Waseda Research Institute for Science and Engineering, Corresponding Author Email: rugbykuribayashi@toki.waseda.jp

virtual environment of a real-world building, based on CARLA [7], which enables us to simulate various sensor data (e.g., LiDAR) from robots. It also contains data gathered from two studies on instructions from sighted individuals. In the first study, instructions were gathered through an online questionnaire by observing a walk-through video from a first-person perspective. This imitates the annotation method used in existing research. The second instruction was collected by conducting an onsite questionnaire that asked sighted passersby to describe the same routes from their memory, which replicates the scenarios envisioned in our study. We observed different characteristics among the two studies in terms of length, number of errors, variety, etc.

Alongside our benchmark, we developed a novel VLN model designed for our scenario defined by Memory-Maze. Given the differences in environments and instruction annotation, directly applying existing supervised models poses a challenge due to their limited performance in unseen settings [9]. In order to realize a scalable navigation robot that could be used in various unseen environments for blind people, our scenario needs to be handled without training or fine-tuning a new VLN model. Hence, we leverage a Large Language Model (LLM) due to its high capability to understand complex natural language and its potential for generalization in the new task without training. Upon receiving an instruction, our VLN model utilizes the LLM to convert the instruction into Python code based on the robot control API (Section III-B) for route navigation. This code generation approach allows low-level commands, such as path-planning for collision avoidance, to supplement our system. Our experiment showed that our model performed satisfactorily on our benchmark while outperforming the previous state-of-the-art method [10]. Through the study, we demonstrated the difficulty of our benchmark and a tendency for onsite instructions to be more difficult for VLN models to handle.

We summarize our contributions below.

- 1) We constructed a benchmark containing the intersection-based virtual environment of a university building and gathered two sets of instructions, one collected by thinking out loud and one obtained from human memory.
- 2) We developed an LLM-based VLN model and evaluated it in the benchmark. We revealed insights regarding the gap between the instructions collected based on memory and those collected thinking out loud.

II. RELATED WORK

A. Assistive Navigation Systems for Blind People

Recently, navigation robots have been explored to use their various sensors to aid blind people to avoid obstacles while navigating [2], [3], [4]. A common practice is to prepare prebuilt maps and infrastructure for localization and manual destination selection [2], [3], [4]. This practice poses a limitation for these systems, as prebuilt maps and infrastructure are costly to obtain and maintain. Consequently, a map-less approach was also proposed [5]. Based on the instruction

from sighted passersby [6], users input navigation directions through the buttons on the robot’s handle. However, because the system needs users to understand and memorize the instructions, high cognitive loads are placed on the users. To address this, our work aims to present a system that directly interprets instructions from sighted passersby and navigates users autonomously to their destinations.

B. Benchmarks in VLN tasks

The VLN task has been conducted in various benchmarks, ranging from indoor [1], [11], [12] to outdoor [8], [13], [14] settings. Most of the instruction annotations of these benchmarks were created by annotators who typed while concurrently observing a virtual environment or by researchers who constructed them manually. This way of obtaining instructions is not suitable for our purpose, as it does not reflect the scenario of people describing routes from their memories. In our case, we gathered natural language instructions through both an online and an onsite study, where the onsite study contains instructions provided from human memories. In addition, most indoor virtual environments do not feature large public areas where blind people navigate, such as shopping malls or university hallways. These areas contain both static and dynamic obstacles and are characterized by the existence of turning points and intersections (Figure 2). A similar environment is Touchdown [8]. However, its map structure is represented by a navigation graph (i.e., an undirected graph that represents navigable points with nodes), whereas we assume no access to navigation graphs. Furthermore, our environment is fully configurable with various static and dynamic obstacles.

C. VLN Models

Researchers have explored solutions for VLN tasks using supervised models [1], [15], [16], which learn through a sequence of observations and actions to take. These supervised models often do not transfer well in unseen environments [9]. With the recent advancements in LLM, researchers have also explored methods that do not require retraining [10], [17], [18], [19], [20]. One such approach was to use LLMs to extract landmarks from instructions and follow chronologically [17], [18], [20]. Another approach was to utilize LLM to flexibly determine actions at each step. NavGPT [10], for instance, is a model that uses LLM iteratively to select the node to navigate to within a navigation graph. Additionally, researchers have explored approaches to utilize the code generation capability of LLM [21], [22]. In the method proposed by Biggie *et al.* [22], given a prebuilt 3D map, images from their robot, and a Python API, the model generates codes that locate a target object [23], map the object’s location on the 3D map, and navigate to the mapped location [22]. While these methods are effective when the given instructions include sufficient landmarks, instructions recalled from memory often contain insufficient landmarks, potentially leading to failure. Furthermore, these methods are limited by the need for a navigation graph or 3D map, which is difficult to construct for every building. To eliminate

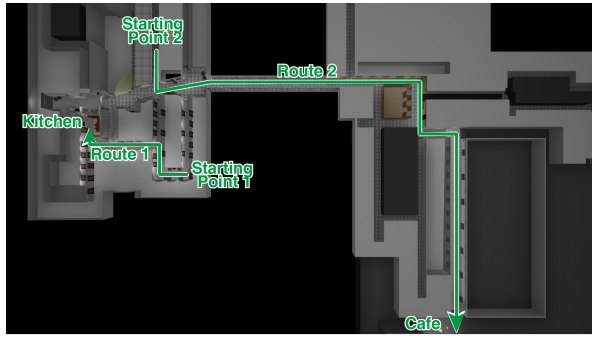


Fig. 2. The bird’s-eye view of the virtual environment and the corresponding routes we used in our studies.

this requirement, models have been proposed to predict navigation graphs [24] or low-level actions [15] iteratively. However, the need for iterative inference prolongs inference time, which may affect navigation by not reacting to dynamic obstacles that appear in the real world responsively. Our model utilizes LLM to produce navigation codes that follow a specified path in a single iteration before the navigation and allows flexible integration of low-level planning algorithms for obstacle avoidance. This direct generation of navigation codes, coupled with existing low-level planning algorithms, allows operation without the need for navigation graphs.

III. MEMORY-MAZE

Here, we describe our benchmark’s virtual environment and the robot simulation program. To simulate our scenario, we selected a floor of a university building, which is characterized by the existence of multiple turning points.

A. Selecting and Building the Simulator

To simulate a scenario where a robot guides a blind person, it is necessary to simulate high-fidelity egocentric visuals that are realistic enough to run an image recognition algorithm. In robot simulation software such as Gazebo [25], it is difficult to create visually detailed environments, which limits the functionality of the image recognition algorithm. Furthermore, simulators used in existing VLN research, such as AI2-THOR [26] and Matterport3D [27], are designed for indoor simulation and are limited in their ability to customize environments and the types of sensors that can be simulated. Thus, we built a novel virtual environment from scratch on top of the CARLA [7] simulator. While primarily developed for autonomous driving simulations, CARLA’s flexibility and compatibility with the Unreal Engine allowed us to create a detailed 3D model of the experimental site. CARLA also offers the ability to configure the existence of static and dynamic obstacles and to simulate various sensors like RGB cameras, depth sensors, and LiDAR sensors.

We created a 3D model of the experimental site using Fusion 360 [28] and imported it into CARLA. This 3D model accurately reproduces the experimental site, both visually and in terms of floor layout. It also includes major objects along the route (doors, chairs, a statue, etc.).

B. Implementation of the Control Program

Our next step was to develop a control program for the robot in the simulator. Utilizing CARLA’s Python API to control the navigation robot, we implemented various control functions. We describe four major functions implemented.

We implemented functions for the agent to move forward (`move_forward(distance)`), find a turning point (`detect_turning_point()`), and turn (`turn(direction)`) using CARLA’s `vehicle.apply_control` API. When using `move_forward(distance)` function, to ensure the robot moves along the path without colliding with walls, we implemented a feature that makes the robot navigate as closely to the center of the corridor as possible. We calculate the central path based on the coordinates of the four corners of the corridor in the 3D model. The central path tracking is realized through PID control, which adjusts the robot’s steering angles. When the `detect_turning_point()` function is used, it determines if the robot is in the pre-annotated areas of turning points and returning navigable directions if the robot is in one of them. Once the robot is at the turning point, it could change its direction using the `turn(direction)` function. In our experiment, coordinates of the corridor’s corners and the turning point areas are acquired from the virtual environment to reduce errors resulting from noise in perception or control and focus on executing instructions. However, these can be obtained using our prior well-established methods [5].

Additionally, we implemented an image recognition module `detect_from_RGB_image(object)`, to manage landmark-related instructions such as “*turn after finding a chair.*” While most existing object detection models are designed to identify objects from predefined classes, they are not capable of detecting arbitrary objects. Therefore, we used Grounding DINO [29], an open-vocabulary object detection model. Open-vocabulary object detection models output bounding boxes for any object by using the object’s name as a query. With the object detection model selected, we then used CARLA’s RGB sensors, positioned on the robot, to capture images. To address tasks requiring the robot to identify an object multiple times (e.g., “*turn after passing four doors*”), we added tracking algorithms to avoid counting the same object in different frames as distinct entities.

We further assume that in instructions that require finding landmark objects, the objects are located in close vicinity. For example, in the instruction “*turn after finding [object],*” although the camera could capture the object at a considerable distance, such instructions typically imply that “[*object*]” is near the robot. Therefore, we utilized the depth sensors available in CARLA to measure the distance to each object in the image, filtering out objects that are far away to ensure only those at close range are detected. We set the distance threshold to be four meters.

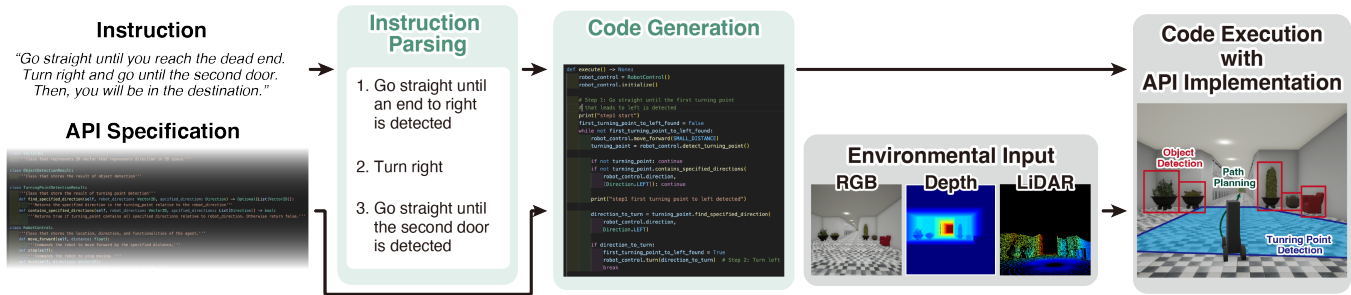


Fig. 5. Overview of our proposed method. Given the instructions from a sighted passerby, an LLM first parses it into itemized format. Then, combined with the API specification, the LLM generates Python code to control the robot, which runs in the virtual environment using the simulated sensor inputs.

found in the samples from the online study. This shows the diversity in the instructions’ wording when described from memory. While the instructions from the online study were translated using LLM, we believe that these results hold with the original instructions. We also manually analyzed each instruction to determine if it contained significant errors, *i.e.*, the number of failures in describing the route correctly. The result is shown in Table I. Reasons for the instructions in the online study that were classified as failures are indicating a wrong direction at a turning point, instructing a turn at an incorrect turning point, and suggesting unnecessary extra turns. For instructions collected in the onsite study, the reasons for the failures were containing extra turns, directing to an incorrect turning point, leading to a wrong destination, lacking essential turn information, instructing to turn to incorrect directions in a turn, and containing inaccurate environmental details. The lack of essential turn information occurred frequently in the instructions of R2. This highlights the difficulty of handling instructions from human memory compared to instructions obtained in a traditional way because instructions from human memories are likely to contain errors.

V. VLN AGENT IMPLEMENTATION

In this section, we describe our prototype VLN model, which is also used to test our benchmark. To satisfy the requirements of our scenario, it contains two characteristics. First, we utilized LLM’s capability to generalize to various tasks and comprehend complex natural language instructions, so that no additional training is required when deployed in a new setting. Second, our method requires a single inference iteration to generate navigation code for robot control, as opposed to existing models that make repeated inferences during navigation, which may prolong navigation time. The generation of navigation code potentially leads to the benefit of integrating existing, well-established methods, such as for obstacle avoidance or turning point detection.

We define the following as inputs to the agent: *natural language instruction*, the *environment input* which includes the details obtained from sensors, *API specification* which includes the commands and their explanations in Python that the agent can use as described in Section III-B, *API implementation* which is the actual implementation of the API specification, and the *initial orientation* of the robot. We assume the initial orientation is known, as the blind user may

adjust it. We used the GPT-4 model for the LLM, which is provided via a public API. For the initial setup of the prompt, instructions from five participants in the online study were used to construct the prompt for the proposed systems, *e.g.*, use it as a few-shot learning prompt. The remaining were used for the evaluation in Section VI. The implementation overview is shown in Figure 5.

A. Parsing Instruction

The system first parses a natural language instruction to step-by-step instructions using LLM. This was done to organize our benchmark’s diverse natural language instruction and make it more interpretable before generating navigation codes. To achieve this, we prompt LLMs with a set of rules they should follow, such as the requirement to describe when and which turning point to turn, and which object the robot should detect, along with examples of possible input and expected output. After parsing, each navigation step is returned as a brief sentence. We employ a two-stage prompting process with the LLM to generate more accurate outputs. Initially, we prompt LLM to provide a thought to guide the generation of the first output. Following this, we prompt LLM to refine the output by incorporating a second thought, leading to the finalized output.

B. Navigation Code Generation

After parsed instructions have been obtained, the LLM now generates the navigation codes in Python. We prompt LLM with an API specification that includes a range of commands for robot operations (*e.g.*, `move_forward(distance)` function). These commands are complete with docstrings of their usage explanation [22], [23] and instructions to generate Python codes that follow the provided specification. For `detect_from_RGB_image(object)`, our model uses an open vocabulary object detector internally (Section III-B) and flexibly determines which object to detect by generating an object argument. The API specification was formatted to the similar format of the previous work [22], [23], but with additional notes, such as how each function should be and not be used. We employ the same two-stage method as in the parsing stage. Finally, we execute the generated code using API implementation given the initial orientation.

VI. EXPERIMENT

A. Baseline

We compare our model against prior methods that exhibit potential zero-shot transfer capabilities, as is the case with our model. Thus, we used NavGPT [10] as a baseline. NavGPT uses both a visual foundation model and an object detector to generate the caption of the surrounding environment. Based on the caption, an LLM is used to decide the next destination within a predetermined navigation graph. The method iterates the above procedure until the LLM decides that the agent has reached the destination. In the original work, 24 images from the agent were used to capture the surrounding environment. We used only four images, capturing front, left, right, and back. We use the same LLM model, GPT-4, as our system for a fair comparison. For the visual foundation model of NavGPT, we use the GPT-4V model, which accepts visual input. For the object detector, we used the Grounding DINO [29], the same detector as our model. We configured the labels of the detector used in NavGPT by using the same objects detected in our model. Additionally, we constructed a navigation graph over the environment, as the NavGPT required one to operate. To construct the navigation graph, we first randomly placed 1,000 coordinates on passable corridors as nodes. Then, we sampled them to ensure that no two nodes were within 2.5 meters of each other. We also added corridor corners as nodes. Edges were created by connecting four adjacent nodes, excluding those obstructed by walls or other nodes. The resulting navigation graph has 265 nodes and 630 edges, with an average edge length of 3.28 meters and an average degree of 2.38. The numbers of nodes in the navigation graph from the starting to the ending node of R1 and R2 were 13 and 43 nodes, respectively. We limit the iterations of NavGPT to two times the node count in the shortest path toward the destination. We set the initial orientation of NavGPT the direction to be heading, *i.e.*, the same initial orientation as our proposed model.

B. Metrics and Conditions

For the metrics, we employ success rate (SR), oracle success rate (OSR), and shortest path distance (SPD) [1], [30], and coverage weighted by length score (CLS) [31]. As CLS computes the similarity of the path on the graph, it requires a dense navigation graph to map the predicted trajectory on to. Thus, we divided passable corridors into 50 cm square grids to serve as nodes on a graph and mapped predicted and ground truth paths onto it to calculate this metric [32]. For the NavGPT and our proposed system, each metric was calculated with and without the instruction parsing module described in Section V-A. While we obtained five instructions that described alternative routes, in this study, we report the metric with respect to one ground truth route, which is the path illustrated in Figure 2.

VII. RESULTS AND DISCUSSION

Table II reports the results of the study.

TABLE II

TABLE SHOWING THE VALUES FOR EACH METRIC.

Condition Method	Route	Online Study Data				Onsite Study Data			
		SR \uparrow	OSR \uparrow	SPD \downarrow	CLS \uparrow	SR \uparrow	OSR \uparrow	SPD \downarrow	CLS \uparrow
NavGPT	1	0.00	0.00	32.75	0.08	0.00	0.00	29.24	0.11
NavGPT with Parser	1	0.00	0.00	28.98	0.10	0.00	0.00	30.38	0.08
Proposed without Parser	1	0.20	0.24	17.01	0.56	0.23	0.33	21.04	0.46
Proposed	1	0.30	0.35	19.66	0.49	0.30	0.38	18.32	0.54
NavGPT	2	0.00	0.00	158.72	0.00	0.00	0.00	162.63	0.00
NavGPT with Parser	2	0.00	0.00	154.65	0.01	0.00	0.00	152.09	0.01
Proposed without Parser	2	0.00	0.00	93.66	0.32	0.03	0.03	117.52	0.20
Proposed	2	0.04	0.04	81.59	0.38	0.03	0.03	98.13	0.29

TABLE III

THE PERFORMANCE TO INSTRUCTION IN EACH ITERATION.

Condition Route	Iteration	Online Study Data				Onsite Study Data			
		SR \uparrow	OSR \uparrow	SPD \downarrow	CLS \uparrow	SR \uparrow	OSR \uparrow	SPD \downarrow	CLS \uparrow
1	1	0.43	0.48	16.37	0.56	0.25	0.40	20.41	0.52
1	2	0.17	0.22	22.94	0.41	0.35	0.35	16.23	0.56
2	1	0.04	0.04	86.82	0.36	0.00	0.00	93.32	0.31
2	2	0.04	0.04	76.36	0.41	0.05	0.05	102.95	0.28

A. Performance of NavGPT and Proposed Method

Overall, we found our model outperforms NavGPT. NavGPT’s suboptimal performance can be attributed to its deviation from the correct direction despite the initial orientation set to be the heading direction and its premature decision that it had reached the goal. This is due to the fact that NavGPT refers to the environment at each inference step with an LLM. If NavGPT makes a mistake even once during this process, it will be challenging for the model to recover back to the correct path. In contrast, our method achieves the desired outcome through one code generation inference, removing the need to make inference at every intermediate step for instructions like “*go straight for 100m and then turn right.*”. We also observed the trend of the instruction parsing module increasing the performance of the two methods.

B. Difficulty of The Benchmark

While the proposed models’ performance between onsite and online instructions was similar in R1, the performance of onsite instructions tended to be lower than that of online instructions. This was particularly true in R2 in terms of SPD and CLS. Similar performances in R1 can be explained by R1’s shorter distance, fewer turns, and participants’ higher self-reported familiarity with the route. The self-reported familiarity rating distribution of R1 shifts slightly more to the right than that of R2. In R1, eight participants answered 7 for the familiarity score (Figure 3). In R2, despite more ratings of 6, it had fewer ratings of 4 and 7 and one rating of 3. As such, humans can better reconstruct R1 in their minds, resulting in fewer memory errors (Table I). The shorter distance and fewer turns of R1 also give the system much space to recover should there be any mismatch between human memories and ground truth. In R2, the route is significantly longer and contains more twists and turns. As shown in Table I, participants commit significantly more mistakes. As a result, it is more likely for the route instructions to contain errors due to human memory and it is harder for the system to recover from errors. This is also evident from the success rates. We verified that the R2 instruction, which our model

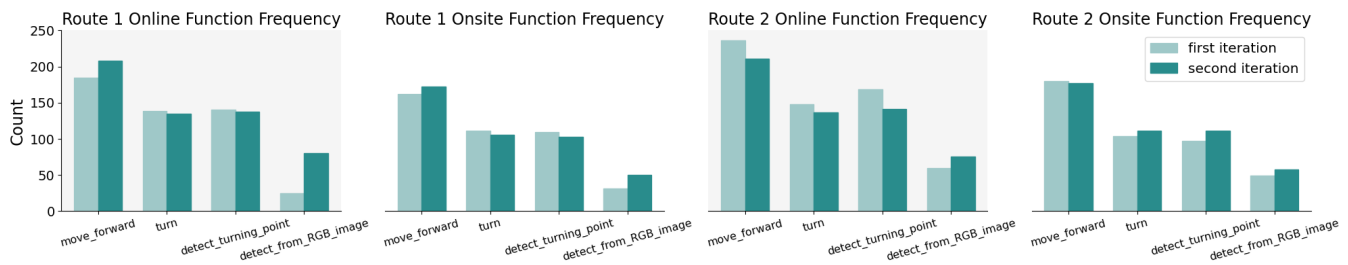


Fig. 6. The figure shows the usage frequency of each function for each experiment condition.

successfully navigated, correctly captured all the turning points and their shape, as well as the accurate locations and types of objects that appeared in the route, which was a rare case among all instructions. Overall, our results demonstrate the difficulty of the instruction data from human memory and the value of our benchmark, particularly our data on R2.

Upon closer inspection, many instructions in our benchmark contained phrases that required a combined understanding of both natural language and the building’s structure, which our proposed model failed to follow. One example was a phrase such as “go along this path and turn right in the first intersection,” which was often described at the starting point of R1. The instruction skips the right turn in the first turning point by describing it as “go along this path,” because the building structure only allows a right turn at the immediate corner. As a result, the instruction starts by describing the first left turn where there are two possible directions to proceed. Similar instructions also frequently appeared to describe the third and fourth turns in R2. While humans can naturally follow such instructions, our model was unable to handle this data, as it explicitly takes into account turning points. This variation in the levels of topological details further highlights the difficulty of our benchmark, which imitates real-world scenarios of blind people seeking navigation instructions.

C. Effect of Refining Instruction

While refining the instruction led to a slight performance improvement in the R2 instruction data collected from the online study, surprisingly, for R1, it decreased the performance of our model. This happened because participants tended to describe more objects during the second iteration, which contained greater variation in object descriptions. R1 also contains much denser objects along the route for participants to describe. Additionally, the short route (and video) allowed participants to re-watch and type in new visible objects, which was not possible in the on-site experiment. For example, one participant described only turning point-related information at the first iteration, while in the second iteration, the participant also described objects to ignore, such as, “then, you will come across an intersection with a door on the left and an intersection with doors on both sides, but ignore them and continue straight ahead.” Figure 6 shows the frequency of usage of each function respective to each condition and iteration. As can be seen from the figure, the increase in the model’s use of `detect_from_RGB` (object)

compared to the first iteration’s usage was particularly significant in online instructions for R1, implying the referral to objects led to the abovementioned decrease in performance. On the other hand, we observed a slight performance increase for the onsite data for both R1 and R2, which suggests the advantage of refining instruction at certain settings. These results highlight the difference between instruction collected traditionally and from memory. The great variation in landmark object descriptions, including the selection of objects and the description of objects further demonstrates the value of our benchmark.

D. Length of Route and Limitation of LLM Usage

For R2, the performance of both models was low. The major reason was the difficulty in handling the input instructions. Apart from what’s mentioned before, longer routes also result in participants tending to describe the lengths inaccurately for certain path segments or not including sufficient information about the destination (Section IV-B).

In R2, we observed the limitation of using LLM. Because the generated codes are long and sometimes contain repetitions, the LLM sometimes stopped generating the navigation code and instead generated a comment in its place, saying that further steps should be implemented by following what’s already implemented (e.g., a line in code saying “# Steps 5 to 8: Implement similar logic for detecting ends and turning points as in steps 1 and 3”). While we tried to address this in the prompt by emphasizing that all code should be generated and an established prompting method [33], this persisted.

VIII. CONCLUSION AND FUTURE WORK

This work proposed Memory-Maze and a VLN model that operates with a single inference, no training, and without a prebuilt map for the first step to utilizing VLN technology for navigation robots for blind people. Our experiment demonstrated that our model could complete the task with satisfactory performance while also outperforming NavGPT. The results also reflect the difficulty of our benchmark. More importantly, we found that realistic instructions collected in the onsite environment, where participants had to rely on human memories, were longer with greater variation in words, and contained more errors compared to the instructions collected online. Through the study with the baseline and our proposed VLN model, we also observed a gap between the instructions collected onsite and those collected in traditional settings, particularly in R2. Upon qualitative

inspection, we observed evidence of the tendency for onsite instruction to be more difficult for the model to handle, such as the ones that required understanding of “go along this path.” This suggests that future works on VLN should consider a more adaptive map representation where nodes and turns are not strictly defined, or a more flexible approach to accommodate varying topological descriptions.

We also observed that the difficulty of the task may be influenced by the method of instruction collection, such as in the case of the second instruction on a short route when collected online. These findings suggest that researchers should exercise caution in future research when considering VLN technology for practical applications, as instructions collected in traditional settings may not fully represent the instructions encountered in real-world scenarios. For future work, we aim to implement additional modules that detect potential errors in the navigation so that the user can ask for the route again. Also, while in this study, we only used instructions from participants, for future practical usage, we aim to also explore the interactive aspect with users and robots. For example, the method could also benefit a blind user, which could guide the instruction from passersby to be better or rephrase it itself, potentially leading to better performance of the robot. We believe that our benchmark based on the scenario of a navigation robot for blind people provides a new perspective to the VLN task, as it contains greater variety in descriptions, is of higher difficulty, and most importantly, reflects a real-world application scenario.

ACKNOWLEDGEMENT

This work was supported by JSPS KAKENHI No. 23KJ2048 and 21H05054.

REFERENCES

- [1] P. Anderson, Q. Wu, D. Teney, J. Bruce, M. Johnson, N. Sünderhauf, I. Reid, S. Gould, and A. Van Den Hengel, “Vision-and-language navigation: Interpreting visually-grounded navigation instructions in real environments,” in *CVPR*. IEEE, 2018, pp. 3674–3683.
- [2] J. Guerreiro, D. Sato, S. Asakawa, H. Dong, K. M. Kitani, and C. Asakawa, “Cabot: Designing and evaluating an autonomous navigation robot for blind people,” in *ASSETS*. ACM, 2019, pp. 68–82.
- [3] S. Liu, A. Hasan, K. Hong, R. Wang, P. Chang, Z. Mizrachi, J. Lin, D. L. McPherson, W. A. Rogers, and K. Driggs-Campbell, “Dragon: A dialogue-based robot for assistive navigation with visual language grounding,” *arXiv preprint arXiv:2307.06924*, 2023.
- [4] S. Kayukawa, D. Sato, M. Murata, T. Ishihara, A. Kosugi, H. Takagi, S. Morishima, and C. Asakawa, “How users, facility managers, and bystanders perceive and accept a navigation robot for visually impaired people in public buildings,” in *RO-MAN*. IEEE, August 2022.
- [5] M. Kuribayashi, T. Ishihara, D. Sato, J. Vongkulbhisal, K. Ram, S. Kayukawa, H. Takagi, S. Morishima, and C. Asakawa, “Pathfinder: Designing a map-less navigation system for blind people in unfamiliar buildings,” in *CHI*. ACM, 2023, pp. 1–16.
- [6] K. Müller, C. Engel, C. Loitsch, R. Stiefelbogen, and G. Weber, “Traveling more independently: A study on the diverse needs and challenges of people with visual or mobility impairments in unfamiliar indoor environments,” *TACCESS*, vol. 15, no. 2, pp. 1–44, 2022.
- [7] A. Dosovitskiy, G. Ros, F. Codevilla, A. Lopez, and V. Koltun, “Carla: An open urban driving simulator,” in *CoRL*. PMLR, 2017, pp. 1–16.
- [8] H. Chen, A. Suhr, D. Misra, N. Snaveley, and Y. Artzi, “Touchdown: Natural language navigation and spatial reasoning in visual street environments,” in *CVPR*, 2019, pp. 12 538–12 547.
- [9] W. Wu, T. Chang, X. Li, Q. Yin, and Y. Hu, “Vision-language navigation: A survey and taxonomy,” *Neural Computing and Applications*, pp. 1–26, 2023.
- [10] G. Zhou, Y. Hong, and Q. Wu, “Navgpt: Explicit reasoning in vision-and-language navigation with large language models,” *arXiv preprint arXiv:2305.16986*, 2023.
- [11] J. Thomason, M. Murray, M. Cakmak, and L. Zettlemoyer, “Vision-and-dialog navigation,” in *CoRL*. PMLR, 2020, pp. 394–406.
- [12] Y. Qi, Q. Wu, P. Anderson, X. Wang, W. Y. Wang, C. Shen, and A. v. d. Hengel, “Reverie: Remote embodied visual referring expression in real indoor environments,” in *CVPR*, 2020, pp. 9982–9991.
- [13] H. De Vries, K. Shuster, D. Batra, D. Parikh, J. Weston, and D. Kiela, “Talk the walk: Navigating new york city through grounded dialogue,” *arXiv preprint arXiv:1807.03367*, 2018.
- [14] Z. Huang, Z. Shangguan, J. Zhang, G. Bar, M. Boyd, and E. Ohn-Bar, “Assister: Assistive navigation via conditional instruction generation,” in *ECCV*. Springer, 2022, p. 271–289.
- [15] J. Krantz, E. Wijmans, A. Majumdar, D. Batra, and S. Lee, “Beyond the nav-graph: Vision-and-language navigation in continuous environments,” in *ECCV*. Springer, 2020, pp. 104–120.
- [16] P. Anderson, A. Shrivastava, J. Truong, A. Majumdar, D. Parikh, D. Batra, and S. Lee, “Sim-to-real transfer for vision-and-language navigation,” in *CoRL*. PMLR, 2021, pp. 671–681.
- [17] D. Shah, B. Osiński, S. Levine, *et al.*, “Lm-nav: Robotic navigation with large pre-trained models of language, vision, and action,” in *CoRL*. PMLR, 2023, pp. 492–504.
- [18] R. Schumann, W. Zhu, W. Feng, T.-J. Fu, S. Riezler, and W. Y. Wang, “Velma: Verbalization embodiment of llm agents for vision and language navigation in street view,” *arXiv preprint arXiv:2307.06082*, 2023.
- [19] W. Huang, P. Abbeel, D. Pathak, and I. Mordatch, “Language models as zero-shot planners: Extracting actionable knowledge for embodied agents,” in *ICML*. PMLR, 2022, pp. 9118–9147.
- [20] P. Chen, X. Sun, H. Zhi, R. Zeng, T. H. Li, G. Liu, M. Tan, and C. Gan, “ a^2 nav: Action-aware zero-shot robot navigation by exploiting vision-and-language ability of foundation models,” *arXiv preprint arXiv:2308.07997*, 2023.
- [21] C. Huang, O. Mees, A. Zeng, and W. Burgard, “Visual language maps for robot navigation,” in *ICRA*. IEEE, 2023, pp. 10 608–10 615.
- [22] H. Biggie, A. Narasimha Mopidevi, D. Woods, and C. Heckman, “Tell me where to go: A composable framework for context-aware embodied robot navigation,” *arXiv e-prints*, pp. arXiv–2306, 2023.
- [23] D. Surís, S. Menon, and C. Vondrick, “Vipergpt: Visual inference via python execution for reasoning,” *arXiv preprint arXiv:2303.08128*, 2023.
- [24] J. Krantz, A. Gokaslan, D. Batra, S. Lee, and O. Maksymets, “Waypoint models for instruction-guided navigation in continuous environments,” in *CVPR*. IEEE, 2021, pp. 15 162–15 171.
- [25] N. Koenig and A. Howard, “Design and use paradigms for gazebo, an open-source multi-robot simulator,” in *IROS*, vol. 3. IEEE, 2004, pp. 2149–2154.
- [26] E. Kolve, R. Mottaghi, W. Han, E. VanderBilt, L. Weihs, A. Herrasti, M. Deitke, K. Ehsani, D. Gordon, Y. Zhu, *et al.*, “Ai2-thor: An interactive 3d environment for visual ai,” *arXiv preprint arXiv:1712.05474*, 2017.
- [27] A. Chang, A. Dai, T. Funkhouser, M. Halber, M. Niebner, M. Savva, S. Song, A. Zeng, and Y. Zhang, “Matterport3d: Learning from rgb-d data in indoor environments,” in *3DV*. IEEE, 2017, pp. 667–676.
- [28] Autodesk, “Autodesk fusion: More than cad, it’s the future of design and manufacturing,” Retrieved in February, 2024 from <https://www.autodesk.com/products/fusion-360/overview>, 2024.
- [29] S. Liu, Z. Zeng, T. Ren, F. Li, H. Zhang, J. Yang, C. Li, J. Yang, H. Su, J. Zhu, *et al.*, “Grounding dino: Marrying dino with grounded pre-training for open-set object detection,” *arXiv preprint arXiv:2303.05499*, 2023.
- [30] J. Gu, E. Stefani, Q. Wu, J. Thomason, and X. E. Wang, “Vision-and-language navigation: A survey of tasks, methods, and future directions,” *arXiv preprint arXiv:2203.12667*, 2022.
- [31] V. Jain, G. Magalhaes, A. Ku, A. Vaswani, E. Ie, and J. Baldrige, “Stay on the path: Instruction fidelity in vision-and-language navigation,” *arXiv preprint arXiv:1905.12255*, 2019.
- [32] G. Ilharco, V. Jain, A. Ku, E. Ie, and J. Baldrige, “General evaluation for instruction conditioned navigation using dynamic time warping,” *arXiv preprint arXiv:1907.05446*, 2019.
- [33] S. M. Bsharat, A. Myrzakhan, and Z. Shen, “Principled instructions are all you need for questioning llama-1/2, gpt-3.5/4,” *arXiv preprint arXiv:2312.16171*, 2023.